# Synchrotron EXAFS and XANES Spectroscopy Studies of Transition Aluminas Doped with La and Cr for Catalytic Applications

Michael V. Glazoff

March 2016

This is an accepted manuscript of a paper intended for publication in a journal. This document was prepared as an account of work sponsored by an agency of the United States Government. Neither the United States Government nor any agency thereof, or any of their employees, makes any warranty, expressed or implied, or assumes any legal liability or responsibility for any third party's use, or the results of such use, of any information, apparatus, product or process disclosed in this report, or represents that its use by such third party would not infringe privately owned rights. The views expressed in this paper are not necessarily those of the United States Government or the sponsoring agency.

Prepared for the U.S. Department of Energy
Office of Nuclear Energy
Under DOE Idaho Operations Office
Contract DE-AC07-05ID14517

The INL is a U.S. Department of Energy National Laboratory operated by Battelle Energy Alliance



# Synchrotron EXAFS and XANES Spectroscopy Studies of Transition Aluminas Doped with La and Cr for Catalytic Applications

Michael V. Glazoff<sup>(1,\*)</sup>

(1) Advanced Process and Decision Systems, Idaho National Laboratory, P.O. Box 1625, MS 3710, Idaho Falls, ID 83415

**Abstract** Transition aluminas doped with Cr find widespread application in the dehydrogenation catalysis industry, while La-stabilized transition aluminas are used extensively for high temperature application as catalytic supports [1]. In this work, detailed synchrotron XAFS-spectroscopy studies were conducted to shed light upon the atomic mechanisms of surface and subsurface reconstructions and/or catalytic support stabilization of doped aluminas. It was demonstrated that in four transition aluminas doped with Cr, it's the atoms are mostly in the state of oxidation Cr<sup>3+</sup> and enter nanoparticles of Crbearing phases (Cr<sub>2</sub>O<sub>3</sub> in the case of gamma- and -chi-alumina). In the transition series aluminas: "gamma - chi - theta eta-alumina" the change of properties (in particular, the dramatic increase of dehydrogenation catalytic activity and catalyst longevity and the coloration of samples) takes place because of the reduction in the average size of Cr clusters and their appearance on the Al<sub>2</sub>O<sub>3</sub> surface, probably responsible for change in catalytic activity. It was demonstrated that in the samples of gamma-alumina doped with La any substantial change in the local coordination of the La atoms takes place only upon heating up to 1400°C. This makes the La-stabilized gamma-alumina a perfect catalytic support for the numerous applications, e.g. catalytic three-way conversion of automobile exhaust gases. This change manifested itself in the form of increased La-O bond lengths and the La coordination number (from 8 to 12). Furthermore, it was demonstrated that the local environment of La in this new La-bearing phase cannot be explained in terms of the LaAlO<sub>3</sub> formation. The absence of the La atoms in the second coordination sphere favors monoatomic distribution of La atoms on grain boundaries, proving that only very small amount of this rare earth material is required to achieve full stabilization. It is inferred that the tendency of

La atoms to get surrounded by oxygen atoms, and also the impossibility of going into the alumina bulk, could be a major reason of the increased thermal stability of gamma alumina doped with lanthanum.

### 1. Introduction

Studies of transition aluminas that can be obtained via the boehmite or bayerite routes (see Figure 1) represent a considerable interest as catalytic supports and catalysts [1, 2]. In order to be used as a catalyst, a material must possess well-developed surface area and a high density of active catalytic sites on such surface [3-5]. Among the many alumina polytypes such materials as gamma-, delta, and theta-aluminas stand out, having specific surface areas >200 m²/g in materials calcined at 1000°C [1]. Unfortunately, as temperature grows, the specific surface area of these materials rapidly goes down because of reactive sintering and phase transformation to the thermodynamically stable alpha-alumina.

In order to retain high specific surface area of catalytic supports at elevated temperatures (>1000°C), dopants must be used preventing the undesirable reactive sintering and phase transformations. Typically such elements as silicon, phosphorus, zirconium, alkaline earth metals (Na, K etc.) rare earth metals (La, Ce, Pr, Nd) and some others are used to achieve this goal. For this reason the study of stabilization mechanism is of key importance for environmental catalysts businesses, because such understanding would allow for the economical solutions ensuring that that the catalyst/catalytic support couple remains active at high temperatures for the extended period of time.

Different opinions were expressed about the physico-chemical nature of the stabilization mechanism. One such possibility would be the formation of a protective layer of an aluminate (not necessarily contiguous), which would slow down the processes of surface diffusion of Al atoms and would prohibit the formation of the thermodynamically stable alpha-alumina phase. Also, La atoms could enter either octahedral or tetrahedral sites in the gamma-alumina defect spinel structure [6]. However, since the atoms of La are

relatively large, both types of processes should not be considered. The situation is different with atoms of Cr, because Cr ionic radii are pretty close to that of  $Al^{3+}$  ( $Cr^{3+}$  - 0.64 Å;  $Cr^{6+}$  - 0.35 Å;  $Al^{3+}$  - 0.57 Å).

Finally, rare earth cations (e.g. La<sup>3+</sup>) could enter into interstitial positions in transition alumina crystalline lattices and, thus, decrease the concentration of oxygen vacancies (the latter typically are formed around the nucleating corundum crystallites). This could also be applicable to different surface phases, because the decrease of the vacancy surface concentration results in slowing down surface diffusion processes critical for the nucleation of the alpha-phase.

EXAFS- and XANES- studies of local atomic coordination and its changes due to different heat treatments gives a possibility to obtain valuable information about the structural and phase composition of dopants in transition aluminas – catalysts and catalytic supports. Such information could be critical for understanding the fundamentals of stabilization mechanism(s) and, consequently, for proposing cost-effective improvements of the transition alumina based catalytic material quality.

This work consisted of two parts: EXAFS studies of the La-stabilized gamma-alumina, and EXAFS- and XANES- studies of Cr dehydrogenation catalyst mounted on the surface of several transition aluminas ( $\gamma$ -Al<sub>2</sub>O<sub>3</sub>,  $\theta$ -Al<sub>2</sub>O<sub>3</sub>,  $\chi$ -Al<sub>2</sub>O<sub>3</sub>, and  $\eta$ -Al<sub>2</sub>O<sub>3</sub>). As such, it represents detailed XAFS spectroscopy data on aluminas doped with Cr and La. Earlier, more general studies employing HRTEM, EELS and ELNES as well as first-principle atomistic simulations were published on this topic [7-9]. The present work should be considered as providing valuable independent information in support of these earlier studies.

### 2. Experimental Part

EXAFS spectra of several samples of transition aluminas discussed above were measured at room temperature at the Institute of Nuclear Physics of the Russian Academy of Sciences (the Novosibirsk Center for Synchrotron Radiation). Synchrotron radiation was properly pre-conditioned using the Si(111) mono-chromator. In order to reduce radiation from higher harmonics a special mirror plated with gold was used. It functioned in the regime of total external reflection [10]. Spectra were measured in the energy range from about 100 eV lower than the absorption edge (which corresponds to 5,483 eV for the La  $L_{III}$ -edge and 5,989 eV – for the Cr K-

edge). Measurements of the absorption fine structure (in both XANES and EXAFS energy ranges) were performed by using X-ray transmission (with ionizing chambers), and also by using excited X-ray fluorescence in the studied samples. At least two spectra were recorded for each sample.

Measurements were performed for a total of 9 samples: a series of 5 samples doped with lanthanum, which included the original sample  $\gamma$ -Al<sub>2</sub>O<sub>3</sub>/La (sample #0) and also samples annealed for 3 hours each at different temperatures: 800°C (#1); 1000°C (#2); 1200°C and 1400°C (#4). The second series consisted of the four samples doped with Cr (catalysts for dehydrogenation catalysis): Cr/ $\gamma$ -Al<sub>2</sub>O<sub>3</sub> catalytic couple – sample #5; Cr/ $\theta$ -Al<sub>2</sub>O<sub>3</sub> (sample #6); Cr/ $\chi$ -Al<sub>2</sub>O<sub>3</sub> (sample #7); and Cr/ $\eta$ -Al<sub>2</sub>O<sub>3</sub> –sample #8. The minimal amount of La sufficient for thermal stabilization of gamma-alumina was described in [9]. The amounts of Cr and the sample preparation technique were covered in detail in [8].

Samples doped with Cr (see Figure 2) were mixed with Vaseline until a fully homogeneous mixture was obtained. This mixture was further placed in between two thin polystyrene films – this technique was used to measure transmission in the case of Cr-bearing samples. A different method (massive blocks) was used for the La-bearing alloys, in which case X-ray fluorescence was measured. Single crystalline powders of  $SrLaAlO_4$  and  $(NH_4)_2Cr_2O_7$  were used as reference substances inasmuch as their atomic structure is very well established.

### 3. Results and discussion

### 3.1 Samples Doped with Cr

A detailed visual inspection of all the four samples doped with Cr was conducted; see Figure 2.One can easily see coloration changes in the row  $Cr/\chi$ -Al<sub>2</sub>O<sub>3</sub> -  $Cr/\gamma$ -Al<sub>2</sub>O<sub>3</sub> -  $Cr/\eta$ -Al<sub>2</sub>O<sub>3</sub> -  $Cr/\eta$ -Al<sub>2</sub>O<sub>3</sub> from light green to dark green to light brown to, finally to dark brown for eta-alumina/Cr catalytic couple. It is known that the coloration of Cr-containing compounds may be different – from yellow/red for  $Cr^{6+}$  (in  $CrO_4^{2-}/Cr_2O_7^{2-}$ , depending on the value of pH) to green - for compounds containing  $Cr^{3+}$ . Consequently, a

change in color might be an indication of transition of Cr to higher valence states (e.g.  $Cr^{6+}$ ). The preferred coordination in this case would be tetrahedral, while  $Cr^{3+}$  cations are typically octahedrally coordinated (for example, in chromia,  $Cr_2O_3$ ).

However, in ruby (corundum doped with  $Cr^{3+}$ ) red coloration is caused by splitting of the *d*-terms by crystalline field.  $Cr^{3+}$  - O bond length changes from 1.965 Å (2.016 Å) to 1.86 Å (1.97 Å)<sup>1</sup>. A substantial distortion of the octahedral coordination of the Cr ions takes place causing as a result, a change in coloration, Figure 3.

With these visual observations in mind, one can turn to the analysis of X-ray absorption spectra. Usually such spectra recorded at the Cr K-absorption edge are characterized by the well-expressed near-edge fine structure (XANES energy range), which is very sensitive to the changes in the local coordination of Cr atoms. For this reason a special attention was paid to the studies in the XANES energy range of the alumina samples doped with Cr. The spectra of the four samples of  $Al_2O_3/Cr$  catalytic couples plus the reference spectrum of the  $(NH_4)_2Cr_2O_7$ , are presented in Figure 4. It clearly indicates that there is a peak for all samples in the XANES energy range, which attains the highest maximum for  $(NH_4)_2Cr_2O_7$ . This spectral line is attributed to the Is - 3d optical transitions, which are prohibited in the dipole approximation [10]. However, when the Cr symmetry differs from octahedral (due to distortions of the lattice etc.) the Cr 3d electronic state can couple with the O 2p-state (the so-called "hybridization process"), and this optical transition becomes allowed. Consequently, the corresponding peak will appear in the X-ray absorption spectrum, in the XANES energy range. This line will be very weak for different compounds of  $Cr^{3+}$  (octahedral coordination). On the contrary, for compounds containing tetrahedral-coordinated ions of  $Cr^{6+}$  this line will be very strong and well pronounced. Thus, by monitoring the intensity of this optical transition line it becomes possible to draw important conclusions about the distortion of the  $Cr^{3+}$  octahedral coordination or about the fraction of Cr atoms in tetrahedral (high oxidation state) coordination. It is generally accepted that as the oxidation degree goes up (from  $3^+$  to  $4^+$  to  $6^+$ ) Cr become more and more tetrahedrally coordinated. Furthermore, this could also point toward an easy and inexpensive way of controlling the degree of a given dehydrogenation catalyst poisoning.

<sup>&</sup>lt;sup>1</sup> There are three atoms of Cr of one type and three –of the other.

The weakest 1s-3d optical transition spectral components were measured for samples of gamma- and chi-alumina (#5 and #7), Figure 4. Bright green coloration of these samples also indicates that in both samples Cr possesses the degree of oxidation 3+. The comparison of the corresponding intensities to those of  $Cr_2O_3$  practically does not yield any substantial differences<sup>2</sup>. This brings us to the conclusion that practically all Cr in samples #5 and #7 is in the  $Cr^{3+}$  state. Moreover, an almost perfect match of the near-edge structure in sample #5 and in  $Cr_2O_3$  (data taken from the literature, [15]) makes one think that Cr is present in this sample in the form of (relatively) large 2D-crystallites of  $Cr_2O_3$ . In sample #7 (chi-alumina) the main structural motif remains the same as in #5, but the local atomic coordination of Cr in that sample is distorted more significantly. This might serve as an indication of the smaller size of  $Cr_2O_3$  particles on the chi-alumina surface.

Samples #6 and #8 (see Figure 2) had light brown and dark brown color, respectively. In complete agreement with this observation, the near-edge components in the X-ray absorption spectra of these materials were much better pronounced. This can be an indication of either more significant distortion of octahedral coordination around the Cr<sup>3+</sup> cations, or of the presence of Cr<sup>6+</sup> cations. In order to select the most adequate explanation, it was necessary to turn to EXAFS spectra analyses.

The synchrotron EXAFS studies of these samples clearly indicated that in all samples the preferential state of Cr atom oxidation was Cr<sup>3+</sup>. Figure 5 represents the Fourier-transforms of the obtained EXAFS spectra. It indicates that the most "perfect" short-range order/structure is characteristic of sample #5 (Cr/gamma-alumina). One can clearly see contributions not only from the 1<sup>st</sup> and 2<sup>nd</sup> coordination spheres, but also from higher order, more distant coordination spheres, at least up to 6Å. For sample #7 (Cr/chi-alumina), contributions of more remote coordination spheres are less significant. This is an indication of increased static distortions of crystalline lattice (the value of the Debye-Waller factor goes up). Nevertheless, since all basic features in EXAFS spectra for these samples practically coincide, one comes to the conclusion that motifs of the local atomic coordination in these samples are quite

\_

 $<sup>^{2}</sup>$  In  $Cr_{2}O_{3}$  near-edge XANES structure appears because of some minor distortions of the octahedral coordination due to the fact that its crystalline structure is that of corundum.

similar. One can also infer that in sample #5 (Cr/gamma-Al<sub>2</sub>O<sub>3</sub>) particles of Cr<sub>2</sub>O<sub>3</sub> are relative large, while in the case of sample #7 (Cr/chi-Al<sub>2</sub>O<sub>3</sub>) they are much smaller.

The quantitative analysis of EXAFS spectra of these two samples yields practically the same  $Cr^{3+}$  - O bond length – 1.99Å. This is a perfect fit with the  $Cr^{3+}$  - O interatomic distances in  $Cr_2O_3$  (3 bonds at 1.965Å and 3 bonds at 2.016Å, [15]). Calculations for the second coordination sphere of sample #5 (Cr/gamma- $Al_2O_3$ ) yield two Cr-Cr distances – 2.61Å and 2.94Å, which is very close to the corresponding values for  $Cr_2O_3$  found in the literature (1 atom at a distance of 2.65Å and 3 atoms at a distance of 2.89Å). Additionally, the agreement between calculated and experimental EXAFS spectra performed under the assumption of  $Cr_2O_3$ -like structural model, was excellent, Figure 6.

Thus, the analyzed data clearly indicates that in both samples (i.e.  $Cr/\gamma$ - $Al_2O_3$  and  $Cr/\chi$ - $Al_2O_3$ ) chromium is mostly present in the form of the  $Cr^{3+}$ -bearing oxide,  $Cr_2O_3$ . These results preclude the appearance of catalytically active Cr atoms on the surface or their inclusion into the bulk. Rather, as follows from the previously conducted atomistic simulations [8, 9] Cr atoms enter the octahedral-coordinated cation positions in the subsurface layer of gamma- and chi-alumina.

The situation is quite different for the samples of  $Cr/\eta$ - $Al_2O_3$  and  $Cr/\theta$ - $Al_2O_3$ . According to results of our EXAFS studies, in both samples the Cr coordination number decreases from 6 to ~4.5, and the  $Cr^{3+}$ -O bond length also slightly decreases to 1.975 – 1.98Å. Some small contributions from higher-order coordination spheres could be observed for the  $Cr/\theta$ - $Al_2O_3$  sample. However, they were almost completely absent in the Fourier transform of the EXAF spectrum of  $Cr/\gamma$ - $Al_2O_3$  (in the crystalline structure of  $Cr_2O_3$  the second coordination sphere consists of four atoms of chromium located at two almost identically similar distances). Our efforts to decipher the structure of the  $Cr/\eta$ - $Al_2O_3$  were not completely successful.

It should be noted that the decrease in the Cr-O bond lengths in the samples of  $Cr/\eta$ - $Al_2O_3$  and  $Cr/\theta$ - $Al_2O_3$  ( $\sim 0.01\text{\AA} - 0.015\text{\AA}$ ) is considerably smaller than the difference between  $Cr^{3+}$ -O and  $Cr^{6+}$ -O bond lengths (which is equal to 0.35Å). Thus the  $Cr^{3+}$  distances are more or less the same for all samples; this is also accompanied by the decrease of coordination number. These two observations

make us believe that in the  $Cr/\gamma$ - $Al_2O_3$  -  $Cr/\phi$ - $Al_2O_3$  -  $Cr/\theta$ - $Al_2O_3$  -  $Cr/\eta$ - $Al_2O_3$  sequence the observed changes in EXAFS spectra of the samples are associated with atoms of Cr appearing on the surface and growing distortions of the Cr local environment. These distortions manifest themselves in the form of the increased intensity of the *1s-3d* optical transition line in the XANES energy range. In principle, this statement does not contradict to the fact of the changed sample colorations, because the coloration of  $Cr^{3+}$ -bearing crystals is determined by the transitions between the *d*-levels of the Cr atom. In turn, their respective locations are very sensitive to the local environment and distortions of atomic structure. This means that the appearance of the red component in the sample colorations (changes from bright green to light green to light brown to dark brown, see Figure 2) can take place for  $Cr^{3+}$  bearing compounds only due to distortions and splitting of the electronic *d*-terms. An example of such coloration change is bright red color of the ruby crystals, Figure. This coloration appears due to the decrease of  $Cr^{3+}$ -O bond lengths to 1.86 Å and 1.97 Å.

### 3.2 Samples Doped with Lanthanum

Several representative X-ray absorption spectra recorded at the La  $L_{III}$ -edge are presented in Figure 7 (they were obtained from data on the X-ray fluorescence of La/ $\gamma$ -Al<sub>2</sub>O<sub>3</sub> samples. Fourier transforms of these spectra are presented in Figure 8. It needs to be pointed out that the reliability and accuracy of all conclusions for La-bearing samples will be lower than for Cr-bearing samples, because the energy range that can be studied in this case is very narrow (the distance between the L<sub>III</sub> and L<sub>II</sub> – edges for La is only ~400 eV).

The analysis of data presented in Figures 7 and 8, along with the comparison of two spectra recorded for each sample (only one of those is represented in Figure 7) gave one a possibility to make the following conclusion. Firstly, in the EXAFS spectrum of the original sample #0 (i.e. not heat treated) two peaks can be observed -one at  $\sim$  2Å and the other at  $\sim$  4Å. Secondly, in samples ##1, 2, and 3 (annealed at 800°C, 1000°C and 1200°C for 3 hours, respectively) only one maximum around  $\sim$  2Å is reproducible. Finally in the EXAFS spectra of sample # 4 (annealed at 1400°C) noticeable oscillations can be seen up to the values of the wave vector

exceeding ~9Å<sup>-1</sup>, while the Fourier transform spectrum has an additional feature around 3.2Å. This is a clear indication of the significant, qualitative changes in the local coordination of La atoms at 1400°C.

The quantitative analysis of synchrotron EXAFS spectra is given below and illustrated by Figures 8 and 9.

## 3.2.1 Original sample #0.

The peak located at  $\sim$ 2 Å in Figure 8 is due to the presence of oxygen atoms at average distances  $\sim$ 2.52 – 2.56 Å, with the coordination number of  $\sim$ 8. However, the fit between experimentally obtained EXAFS spectra and those calculated under the assumption that all oxygen atoms are located at the same distance from the central (reference) atom, is not very good. Much better agreement was obtained if one assumed that there are two different La-O bond lengths. The best fit was obtained at 2.47 Å and 2.68 Å. However, the underlying mathematical problem is ill-posed (in the sense of Hadamard, [16]) and over-determined, because to obtain this solution 7 parameters were varied, which exceeded the total number of independent parameters in the experimental data (equal to 4.5-5). This happened due to the limited energy range defined by the difference between  $L_{III}$  and  $L_{II}$  La absorption edges noted above. As a result, the corresponding solution was unstable with respect to small perturbations in the input experimental data [16]. The peak at  $\sim$ 4 Å can be relatively well described under the assumption that there are two principal contributions to this coordination sphere – one from  $\sim$ 12 atoms of oxygen at a distance of 4.38 Å and the other from a somewhat larger number of the Al atoms. The distance distribution function for the latter for these Al atoms is a broad Gaussian curve with the maximum around 4.53 Å.

### 3.2.2 Samples annealed at 800°C (#1), 1000°C (#2) and 1200°C (#3)

The quantitative analysis of EXAFS spectra obtained for these samples yields the following conclusions. Atoms of La in these samples are surrounded by  $\sim$ 8 atoms of oxygen at average distances  $\sim$ 2.49 Å - 2.64 Å. This is close to the result obtained for the sample #0. As in the case of the sample #0, the agreement between experiment and structural model calculations was not very good, for the same reasons. In particular, the solution with two different types of oxygen atoms was the optimal, similar to sample #0 (with the same precautions about the ill-posed problem of the underlying fitting described above)

### 3.2.3 Sample annealed at 1400°C (#4)

The profound changes in the EXAFS spectrum recorded for this sample in comparison to samples #0, #1, #2 and #3, are an indication that annealing at the high temperature of 1400°C causes a phase transformation accompanied by the appearance of a new La-bearing phase. The average La-O distances are higher (2.71 Å –2.73 Å), coordination number for the first coordination sphere increases up to ~12, and a signal from ~6 atoms of Al appears in the second coordination sphere, Figure 9. For this sample the agreement between experiment and calculation is excellent (modeling was done under the assumption that all atoms from the 1<sup>st</sup> coordination sphere are at the same distances from the central atom of La, while the 2<sup>nd</sup> coordination sphere is comprised mostly of Al atoms, see Figure 8. It is important to note that this La-bearing phase is not LaAlO<sub>3</sub>: for the latter, atoms of Al must be located closer to the reference La atom (~3.28 Å). Additionally, the contribution from 6 atoms of La at ~3.79 Å is clearly observed. To repeat, this was not the case for the La-bearing phase discussed above. On the contrary, for sample #4 average positions of La atoms practically do not change. This may be an indication that even after the heat treatment at 1400°C for 3 hours La atoms do not form any new precipitates/agglomerates (i.e. they are located at sufficiently large distances from each other).

Let us discuss the results related to the local atomic environment of La in  $\gamma$ -Al<sub>2</sub>O<sub>3</sub> (La). La coordination numbers observed for samples ##0-3 are too large to be explained in terms of La entering either tetrahedral- or octahedral-coordinated positions in a transition Al<sub>2</sub>O<sub>3</sub> lattice. Indeed, the atoms of rare earth metals for which the atomic diameter is much larger than that of Al, can form oxides and fluorides characterized by high values of the respective coordination numbers [10]. For example, AlF<sub>3</sub> has a rhombohedral - distorted ReO<sub>3</sub> crystalline lattice with coordination number equal to 6. On the other hand, LaF<sub>3</sub> has the tysonite crystalline structure with the coordination number of 12. For this reason it is not surprising that in the present work La coordination numbers in the range from 8 to 12 were established. Such high coordination numbers are an indication that the La nearest atomic environment is qualitatively different from that in Al, and that atoms of La cannot enter the densely packed lattice formed by oxygen atoms (ions). In turn, this might imply that the stabilizing action of La upon the structure of gamma-alumina might be associated with this inability of La atoms to go into the bulk, and to be located individually on grain boundaries and/or other interfaces. Since atoms of La require a

local environment highly enriched with oxygen, they can effectively retard the process of reactive sintering accompanied by grain growth and gamma-to alpha phase transformation.

### 4. Conclusions

- It has been demonstrated that in the samples of different transition aluminas doped with Cr, the atoms of chromium are mostly in the state of oxidation Cr<sup>3+</sup> and enter nanoparticles of Cr-bearing phases (Cr<sub>2</sub>O<sub>3</sub> in the case of gamma- and –chi-alumina;
- In transitional aluminas of the types: "gamma chi theta eta-alumina" the change of properties (in particular, of coloration of samples) takes place because of dramatic reduction in the average size of Cr clusters and, possibly, their appearance on the Al<sub>2</sub>O<sub>3</sub> surface. This has profound implications for catalysis discussed elsewhere [9];
- It was also demonstrated that the substantial change in the local coordination of La atoms in samples of the gamma-alumina doped with La takes place only upon heating up to 1400°C. This change manifested itself in the form of increased La-O bond lengths and the La coordination number (from 8 to 12). It was proved that the local environment of La in this new Labearing phase cannot be explained in terms of the LaAlO<sub>3</sub> formation;
- The absence of the La atoms in the second coordination sphere favors monoatomic distribution of La atoms on grain boundaries;
- It is inferred that the tendency of La atoms to get surrounded by oxygen atoms, and also the impossibility of going into the bulk of alumina crystal, could be a major reason of the increased thermal stability of gamma alumina doped with lanthanum.

### **Acknowledgements**

The author would like to express his sincere gratitude to Prof. Alexander Lebedev of the M.V. Lomonosov Moscow State University, for help with processing of XAFS spectra, and to Dr. John W. Novak, Jr., (Pacific Industrial Development Corporation, formerly of BASF), for his corrections and valuable recommendations. Access to the Novosibirsk Synchrotron Facility (Russian Academy of Sciences) for EXAFS- and XANES-spectroscopy work is also gratefully acknowledged.

This manuscript has been authored by Battelle Energy Alliance, LLC under Contract No. DE-AC07-05ID14517 with the U.S. Department of Energy. The United States Government retains and the publisher, by accepting the article for publication, acknowledges that the United States Government retains a nonexclusive, paid-up, irrevocable, world-wide license to publish or reproduce the published form of this manuscript, or allow others to do so, for United States Government purposes.

### Literature

- 1. K. Wefers, C. Misra, Oxides and Hydroxides of Aluminum (Alcoa Laboratories, Pittsburgh, 1987)
- 2. T. K. Phung, A. Lagazzo, M.Á.R. Crespo, V.S. Escribano, G. Busca, A study of commercial transition aluminas and of their catalytic activity in the dehydration of ethanol, *J. of Catalysis*, vol. 311, pp. 102–113 (March 2014)
- 3. G. Busca, Heterogeneous Catalytic Materials: Solid State Chemistry, Surface Chemistry, and Catalytic Behavior, p.143, Surface Chemistry of Aluminas, Elsevier, Amsterdam (2014)
- 4. J. R. H. Ross, Heterogeneous Catalysis: Fundamentals and Applications, Elsevier, Amsterdam (2012)
- 5. C. N. Satterfield, Heterogeneous Catalysis in Practice (McGraw Hill, New York, 1980)
- 6. Jens K. Nørskov, Frank Abild-Pedersen, Felix Studt, and Thomas Bligaard, Density functional theory in surface chemistry and catalysis, *Proc. Nat. Acad. Sci. USA*, vol.108, No.3, pp. 937-943 (Nov.2010)
- 7. A.Y. Borisevich, S. Wong, S.N. Rashkeev, M.V. Glazoff, S.J. Pennycook, S.T. Pantelides, Dual Nano-Particle/Substrate Control of Dehydrogenation Catalysis, *Advanced Materials*, vol.19, pp. 2129-2133 (2007)
- 8. S. Wang, A.Y. Borisevich, S.N. Rashkeev, M.V. Glazoff, K. Sohlberg, S.J. Pennycook, and S.N. Pantelides, Dopants Adsorbed As Single Atoms Prevent Degradation of Catalysts, *Nature Materials*, vol.3 (3), pp.143-146 (2004)

- 9. M.V. Glazoff, J.W. Novak, Jr., and A. Vertegel, "Thermally Stable Alumina Particulates", US Patent 6764672, July 20, 2004
- 10. A. Grunes, Study of the *K*-edges of 3*d*-transition metals in pure and oxide form by x-ray-absorption spectroscopy, *Physical Review B*, vol. 27, p.2111 (1983)
- 11. J. Stoehr, L.I. Johansson, S. Brennan, M. Hecht, J.N. Miller, Surface Extended X-Ray Absorption Fine Structure Study of Oxygen Interaction With Aluminum (111) Surfaces, *Phys. Rev. B*: *Condens. Matter*, vol.22, pp.4052-4065 (1980).
- 12. Synchrotron Radiation. Properties and Applications. Ed. by K. Kunz, New York, Wiley (1979)
- 13. "X-ray Absorption: Principles, Applications, Techniques of EXAFS, SEXAFS, and XANES, D. C. Koningsberger, R. Prins, A. Bianconi, P.J. Durham, Series: Chemical Analysis, vol.92, John Wiley & Sons (1988)
- 14. Matthew Newville (Consortium for Advanced Radiation Sources University of Chicago, Chicago, IL), Fundamentals of XAFS, Revision 1.7 July 23, 2004
- 15. Inorganic Crystal Structure Database, NIST (2013)
- 16. A.N. Tikhonov and V. Ya. Arsenin, Solutions of Ill-Posed Problems, Halsted Press, New York (1977)

## **Figure Captions**

Figure 1 Transformation sequences of transition aluminas – after Wefers and Misra [1]

Figure 2 Cr catalyst mounted on the surface of different transition aluminas:  $\chi$ -Al<sub>2</sub>O<sub>3</sub>,  $\gamma$ -Al<sub>2</sub>O<sub>3</sub>,  $\theta$ -Al<sub>2</sub>O<sub>3</sub>,  $\eta$ -Al<sub>2</sub>O<sub>3</sub>. Note **change in coloration** (from right to left): light green - dark green - gray - dark brown.

Figure 3 Coloration of different chromium-bearing aluminas

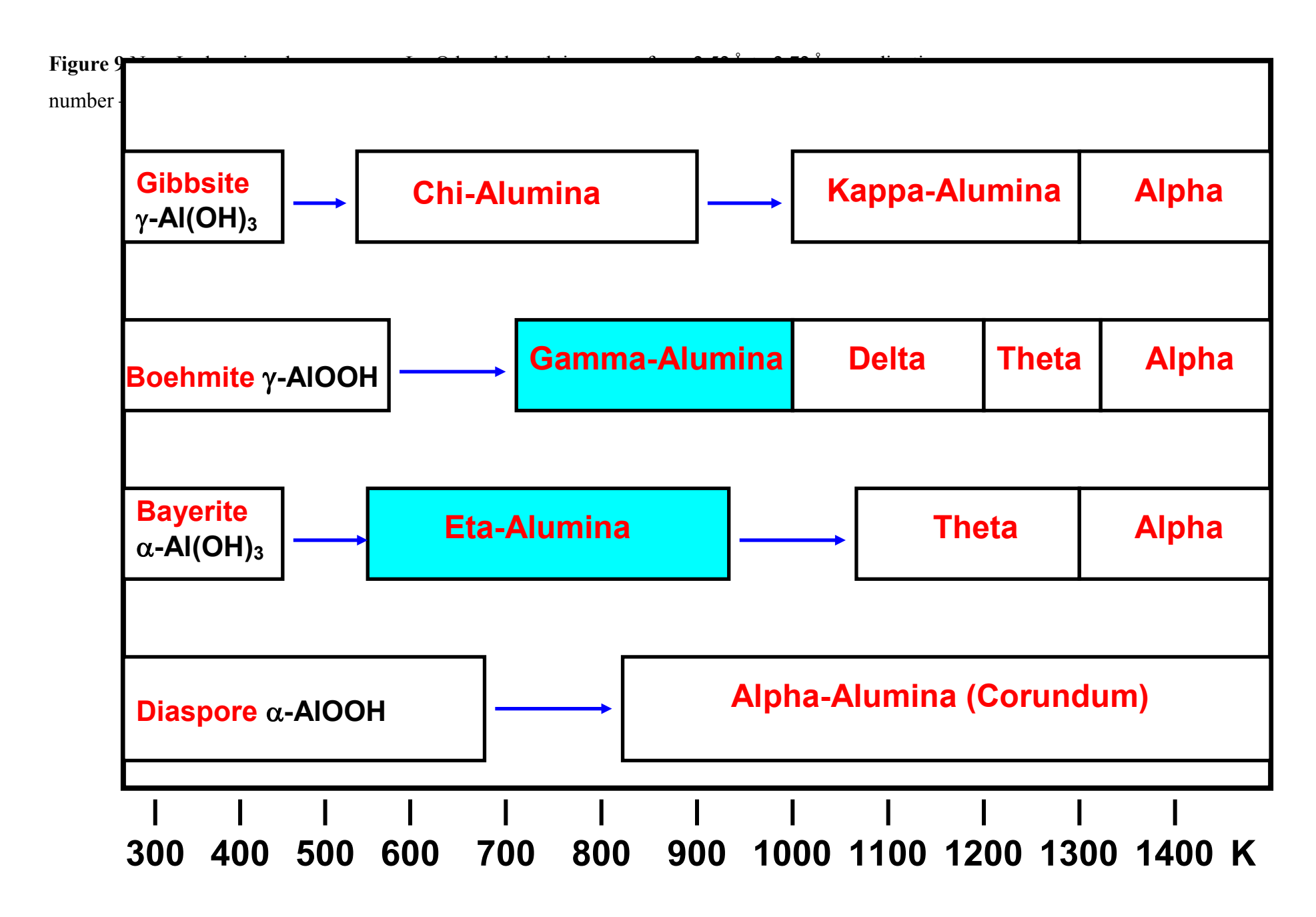
**Figure 4** Absorption spectra of  $\eta$ -,  $\theta$ -,  $\gamma$ -,  $\chi$ -Al<sub>2</sub>O<sub>3</sub> and (NH<sub>4</sub>)<sub>2</sub>Cr<sub>2</sub>O<sub>7</sub> (for reference) clearly displaying peaks in the XANES energy range

Figure 5 Fourier-transforms of EXAFS spectra for different Cr/Al<sub>2</sub>O<sub>3</sub> catalytic couples

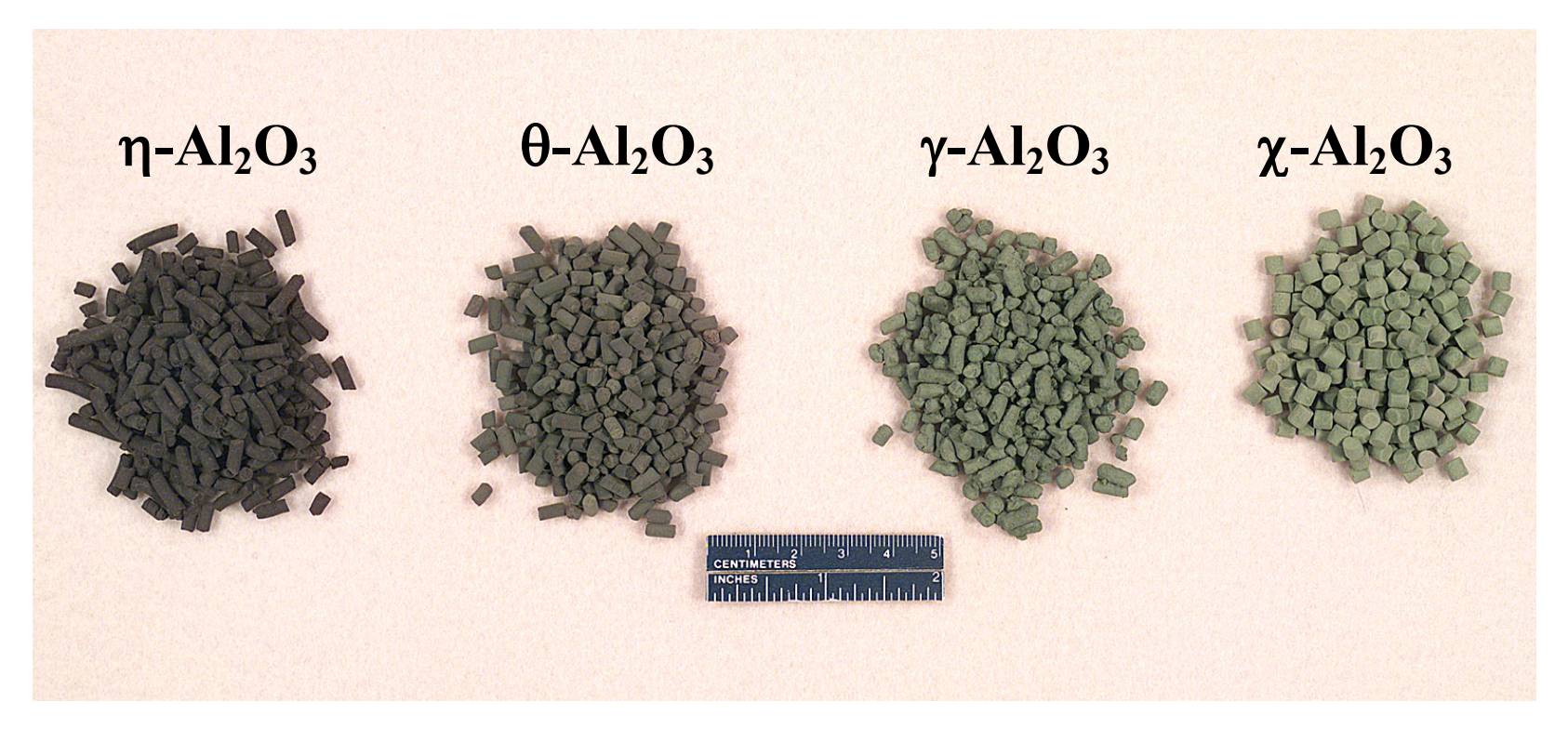
**Figure 6** Computer simulation of EXAFS spectrum for  $\gamma$ -alumina gives a perfect fit with the crystalline structure of Cr<sub>2</sub>O<sub>3</sub> (reciprocal space)

Figure 7 Synchrotron X-ray absorption spectra for several samples of  $La/\gamma$ -Al<sub>2</sub>O<sub>3</sub> recorded at the La L<sub>III</sub> edge

**Figure 8** Synchrotron EXAFS spectra of five La/ $\gamma$ -Al<sub>2</sub>O<sub>3</sub> samples and SrLaAlO<sub>4</sub> in the direct space; note the lack of atomic coordination for all samples except #4 annealed at 1400°C –no La clustering!



**Figure 1** Transformation sequences of transition aluminas (from K.Wefers & C.Misra, *Alcoa Technical Paper No.19*, 1987, [1])



**Figure 2** Cr catalyst mounted on the surface of different transition aluminas:  $\chi$ -Al<sub>2</sub>O<sub>3</sub>,  $\gamma$ -Al<sub>2</sub>O<sub>3</sub>,  $\theta$ -Al<sub>2</sub>O<sub>3</sub>,  $\eta$ -Al<sub>2</sub>O<sub>3</sub> Note change in coloration (from right to left): light green - dark green - gray - dark brown

# **Coloration of Cr compounds**

Cr<sup>6+</sup>- yellow or red, depending on pH; preferred coordination is <u>tetrahedral</u>

Cr<sup>3+</sup>- green, but only in perfect <u>octahedral</u> coordination!



However, in ruby (corundum + Cr<sup>3+</sup>) red coloration is caused by splitting of the <u>d</u>-terms by crystalline field; Cr<sup>3+</sup>-O bond length changes from 1.965 (2.016) Å to 1.86 (1.97)Å For comparison, the Cr<sup>6+</sup>-O bond length is 1.615 Å

<u>Conclusion</u>: changes in color from green to red may be caused <u>either</u> by <u>increased Cr valence</u> state (e.g.  $Cr^{3+} \rightarrow Cr^{6+}$ ) or by <u>distortion of perfect octahedral coordination</u> in  $Cr^{3+}$  compounds

Figure 3 Coloration of chromium compounds

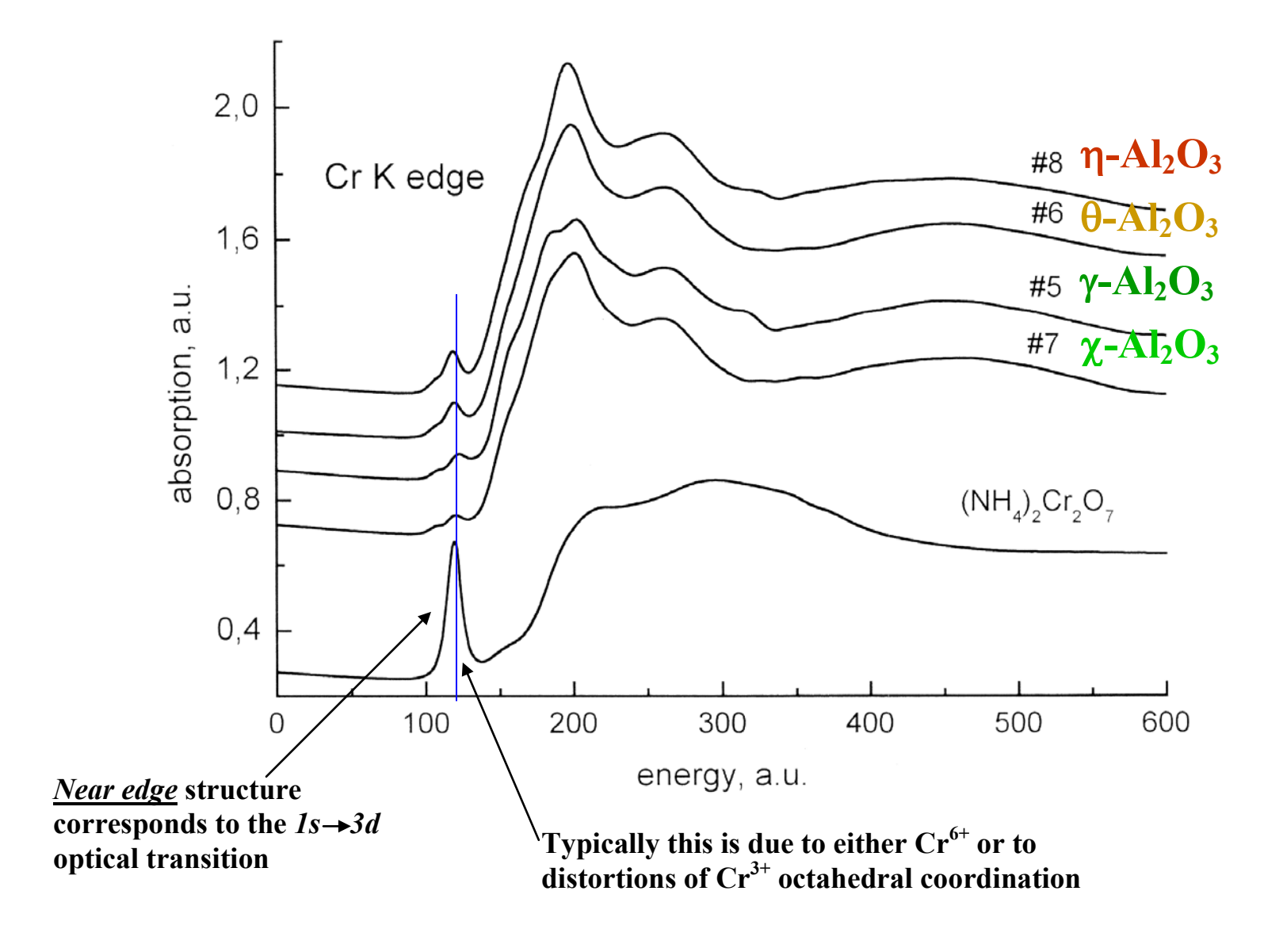


**Figure 4** Absorption spectra of  $\eta$ -,  $\theta$ -,  $\gamma$ -,  $\chi$ -Al<sub>2</sub>O<sub>3</sub> and (NH<sub>4</sub>)<sub>2</sub>Cr<sub>2</sub>O<sub>7</sub> (for reference) clearly displaying peaks in the XANES energy range

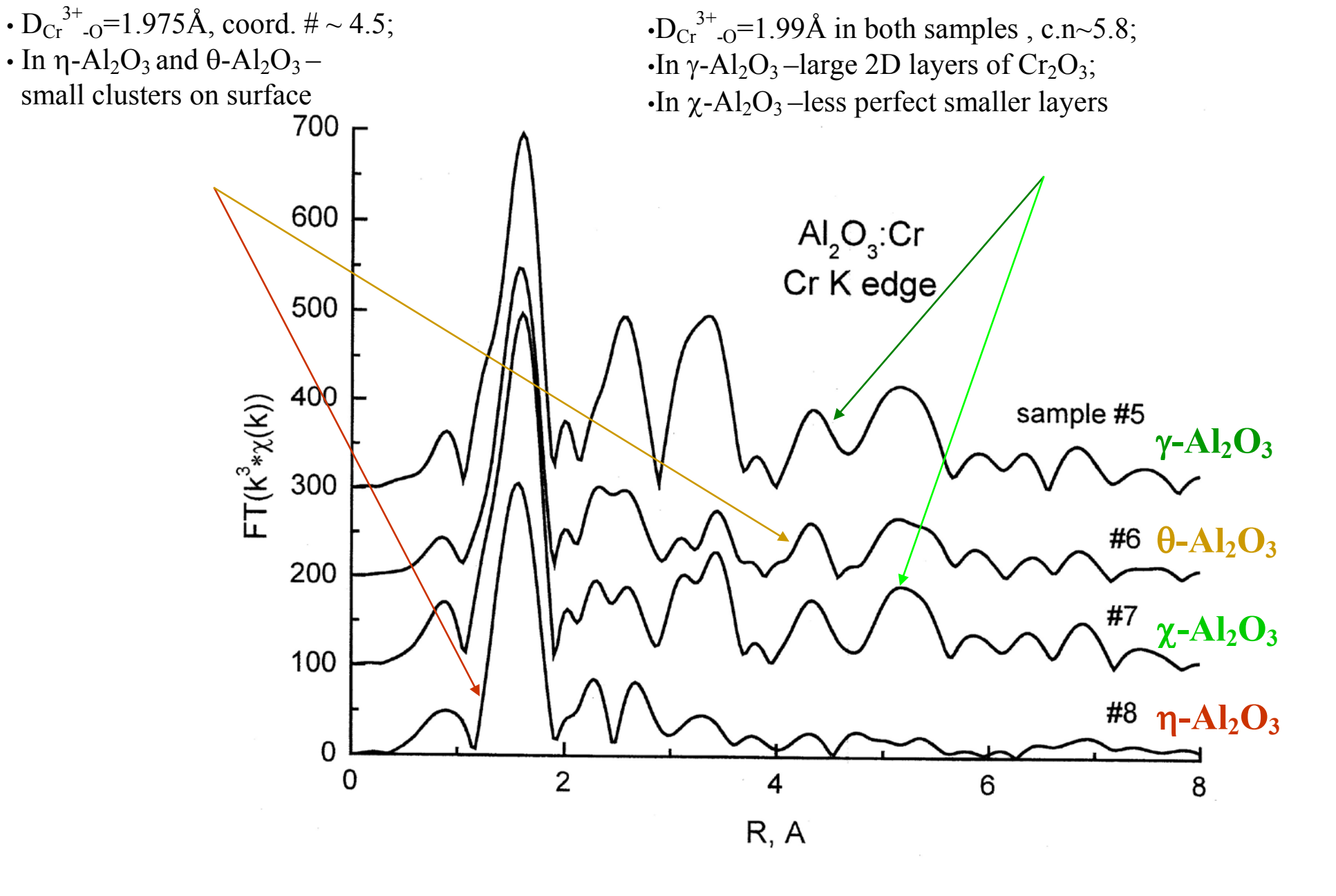
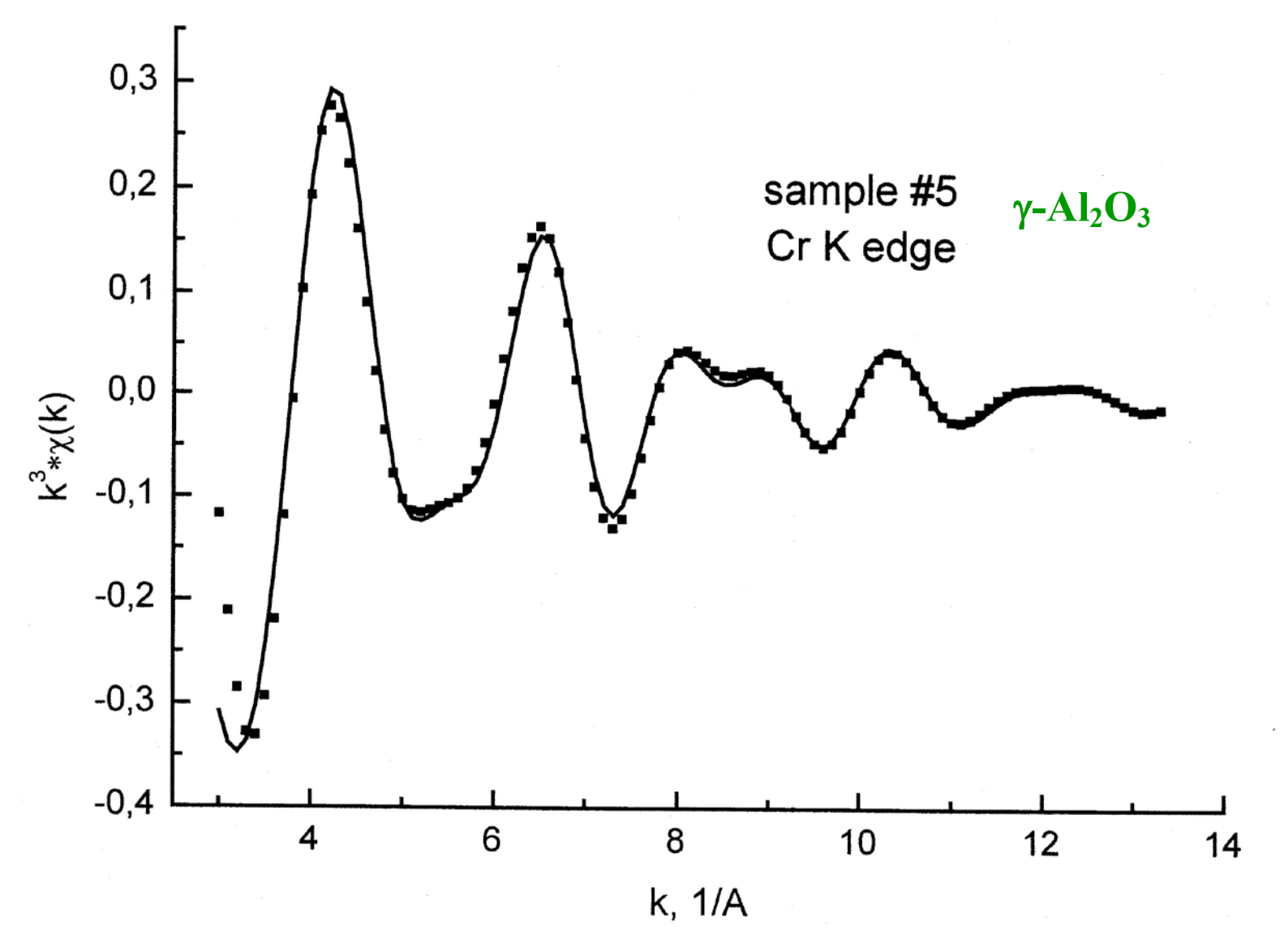


Figure 5 Fourier-transforms of EXAFS spectra for different catalytic couples



**Figure 6** Computer simulation of EXAFS spectrum for γ-alumina gives a perfect fit with the crystalline structure of Cr<sub>2</sub>O<sub>3</sub> (reciprocal space). Solid line –computer simulation; filled squares –experimental data

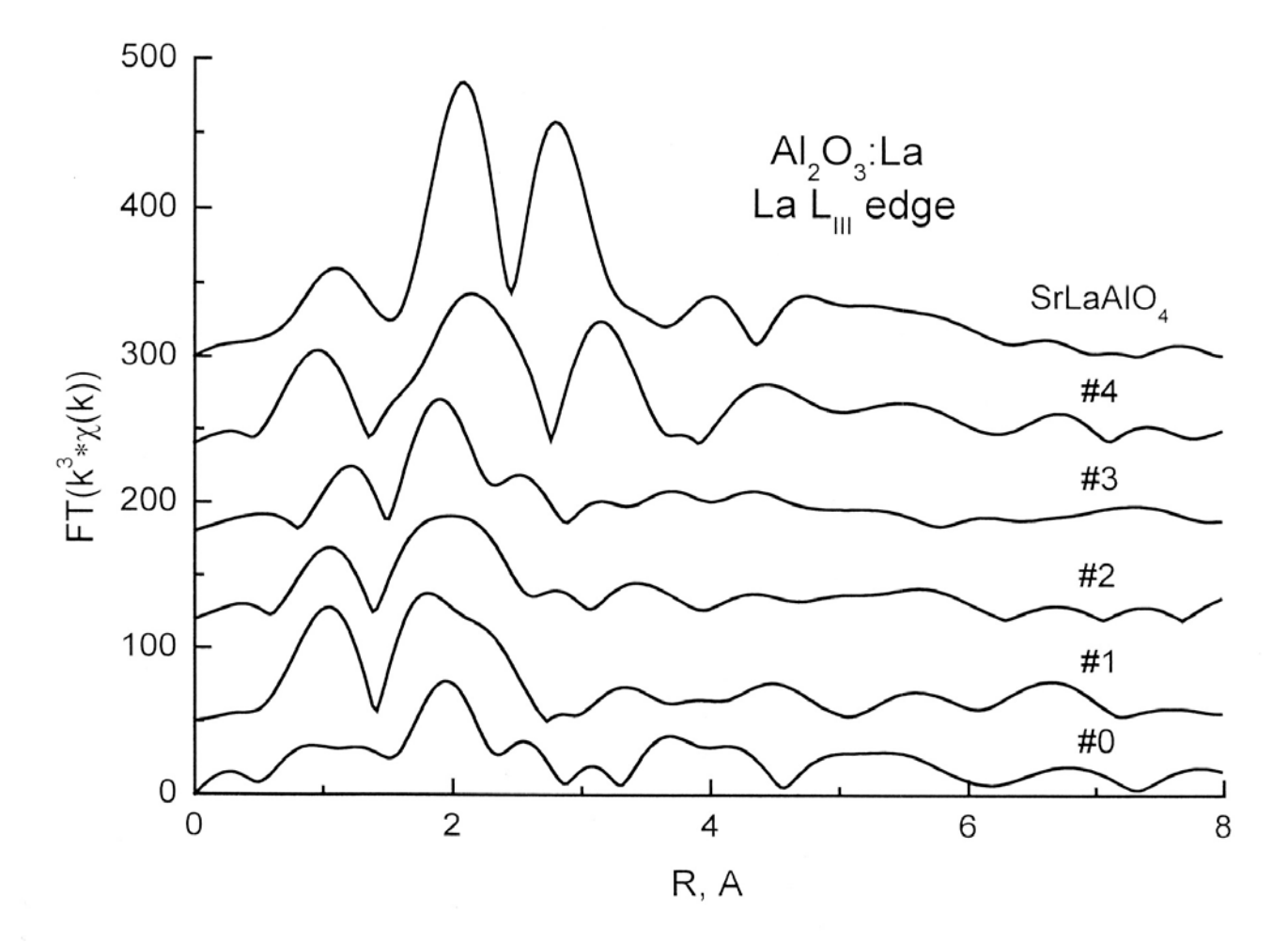
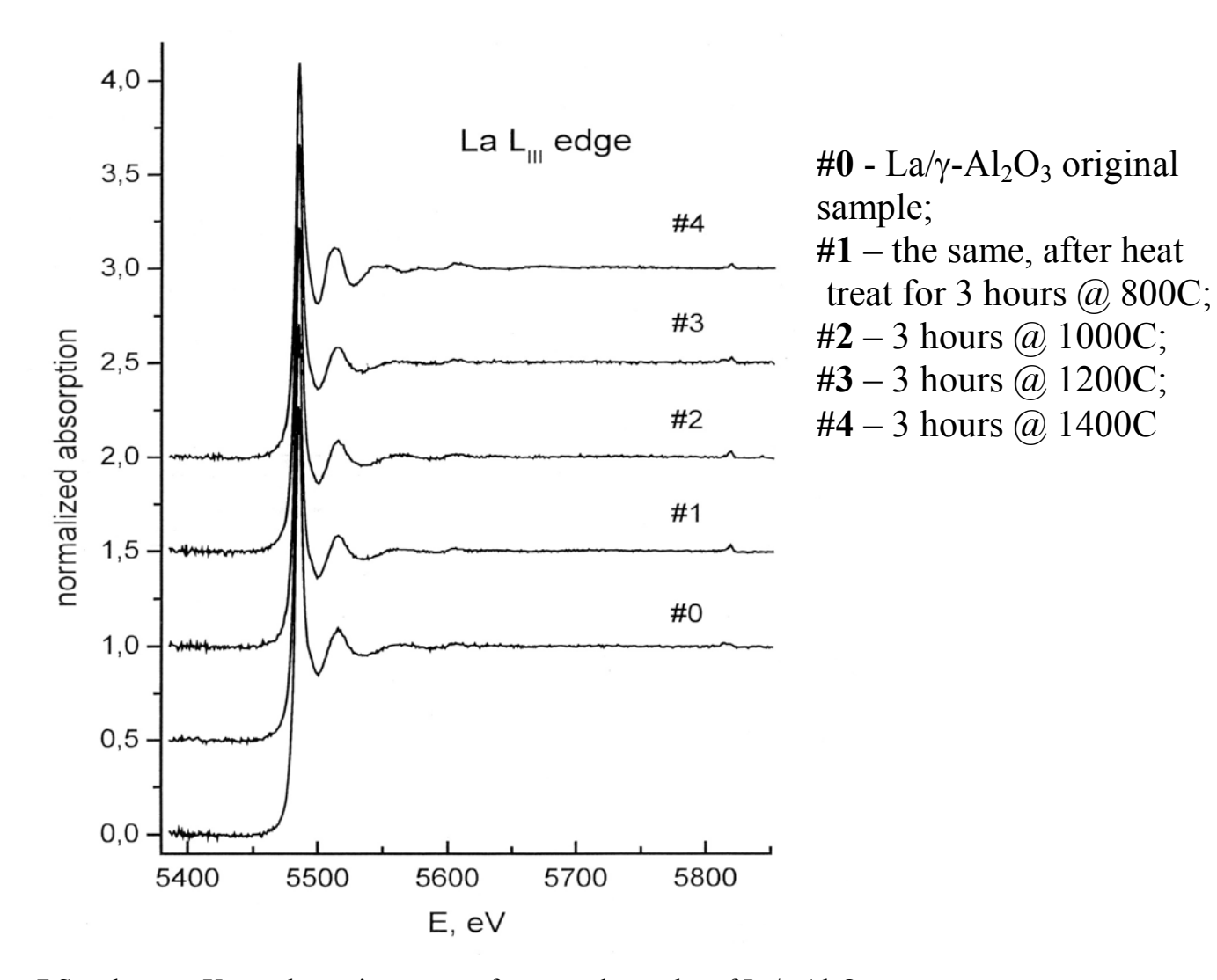
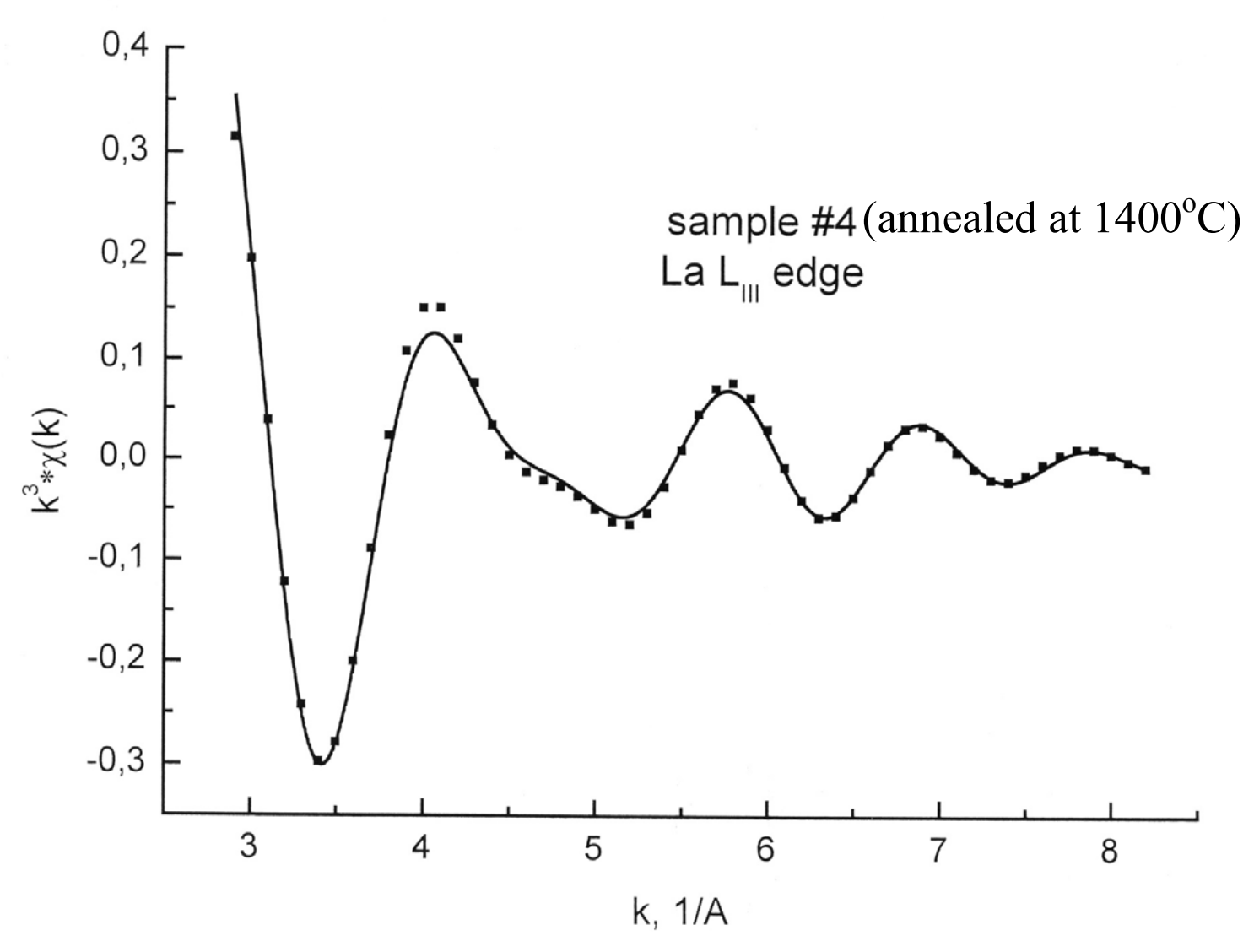


Figure 8 Synchrotron EXAFS spectra of five La/γ-Al<sub>2</sub>O<sub>3</sub> samples and SrLaAlO<sub>4</sub> in the direct space; note the lack of atomic coordination for all samples except #4 annealed @ 1400°C –no La clustering!

#0 - La/ $\gamma$ -Al $_2$ O $_3$  original sample; #1 – the same, after heat treat for 3 hours @ 800C; #2 – 3 hours @ 1000C; #3 – 3 hours @ 1200C; #4 – 3 hours @ 1400C



**Figure 7** Synchrotron X-ray absorption spectra for several samples of  $\text{La}/\gamma\text{-Al}_2\text{O}_3$  recorded at the La  $\text{L}_{\text{III}}$  edge



**Figure 9** New La-bearing phase appears: La-O bond length increases from 2.52Å to 2.72Å; coordination number – from 8 to 12; 1<sup>st</sup> coordination sphere – 12 O atoms; second – 6 Al atoms at 3.55Å. Solid line – computer simulation; Filled squares – experimental points